

Closed-form aftershock reliability of damage-cumulating elastic-perfectly-plastic systems

Iunio Iervolino^{1,*}, Massimiliano Giorgio² and Eugenio Chioccarelli¹

¹Dipartimento di Strutture per l'Ingegneria e l'Architettura, Università degli Studi di Napoli Federico II, Naples, Italy

²Dipartimento di Ingegneria Industriale e dell'Informazione, Seconda Università degli Studi di Napoli, Aversa, Italy

SUMMARY

Major earthquakes (i.e., *mainshocks*) typically trigger a sequence of lower magnitude events clustered both in time and space. Recent advances of seismic hazard analysis stochastically model aftershock occurrence (given the main event) as a nonhomogeneous Poisson process with rate that decays in time as a negative power law. Risk management in the post-event emergency phase has to deal with this short-term seismicity. In fact, because the structural systems of interest might have suffered some damage in the mainshock, possibly worsened by damaging aftershocks, the failure risk may be large until the intensity of the sequence reduces or the structure is repaired. At the state-of-the-art, the quantitative assessment of aftershock risk is aimed at *building tagging*, that is, to regulate occupancy. The study, on the basis of *age-dependent* stochastic processes, derived closed-form approximations for the aftershock reliability of simple nonevolutionary elastic-perfectly-plastic damage-cumulating systems, conditional on different information about the structure. Results show that, in the case hypotheses apply, the developed models may represent a basis for handy tools enabling risk-informed tagging by stakeholders and decision makers. Copyright © 2013 John Wiley & Sons, Ltd.

Received 16 January 2013; Revised 27 July 2013; Accepted 11 August 2013

KEY WORDS: performance-based earthquake engineering; time-variant risk; cumulative damage process; gamma-distributed increments; energy-based damage indices

1. INTRODUCTION

Short-term risk assessment, that is, at the time-scale of weeks/months around a major event, is gathering increasing research attention due to the compelling need of decision makers for quantitative tools enabling to manage such a risk. Of particular interest is the evaluation of the failure probability for mainshock-damaged structures exposed to the following aftershock sequence. This may be referred to as *building tagging* and allows to monitor the variation of structural risk due to both increased vulnerability, caused by cumulative damage, and time-decaying aftershock hazard, and to decide whether to prohibit access to anyone (i.e., *red tag*), allow access only to trained agents for emergency operations (i.e., *yellow tag*), or to resume from business interruptions allowing normal occupancy (i.e., *green tag*). Seminal research on the topic is that of Yeo and Cornell [1–3], who developed aftershock probabilistic seismic hazard analysis (APSHA) and then coupled it with state-dependent fragilities in a performance-based approach to aftershock risk.

Starting from APSHA and background models for aftershock occurrence, this study derives closed-form reliability solutions for elastic-perfectly-plastic (EPP) single degree of freedom (SDOF) systems exposed to post-mainshock seismic hazard. The cumulative damage is described by a stochastic process in which time of occurrence, ground motion intensity, and structural damage produced by each aftershock are all treated as

*Correspondence to: Iunio Iervolino, Dipartimento di Strutture per l'Ingegneria e l'Architettura, Università degli Studi di Napoli Federico II, via Claudio 21, 80125, Naples, Italy.

†E-mail: iunio.iervolino@unina.it

random variables (RVs). Damage increments (i.e., damages in individual seismic shocks) are addressed in the case they are independent and identically distributed (i.i.d.) RVs. It is shown that such hypotheses may apply for simple, yet general, EPP-SDOF systems, considering energy-based damage measures. Increments characterizing the damage process are then assumed to be probabilistically described by a *gamma* distribution, which enjoying the reproductive property enables to obtain a closed-form solution for the probability of failure conditional to a given number of shocks. This leads to retain closed-form also for the reliability assessment in terms of absolute (or unconditional) probability, when the latter is approximated by the probability of failure given the expected number of aftershocks in the time frame of interest. Similarly, approximations of the conditional probability of failure may also be obtained in the following two cases: (i) when it is known that the structure is still surviving at a certain time yet with unknown residual seismic capacity and (ii) when the structure has survived a given number damaging aftershocks of unknown effect. All the models also explicitly account for the fact that the majority of aftershocks are expected to feature insufficient intensity to procure any damage.

The following is structured such that essentials of APSHA of relevance for the developed models are reviewed first. Then, the damage indices and collapse criteria are briefly reviewed. Subsequently, the structural cumulative degradation stochastic process, based on the hypothesis that damage increments are independent and identically gamma-distributed, is addressed and time-variant reliability formulations are derived. Finally, an application, referring to an EPP-SDOF supposed to be exposed to a generic aftershock sequence from a magnitude, M , 6.3 event is developed to illustrate the derived models and their possible use for building tagging.

2. AFTERSHOCK PROBABILISTIC SEISMIC HAZARD ANALYSIS ESSENTIALS

This section only recalls those essential results of APSHA, which are required by the models derived in Section 4, while the reader should refer to [1] for further details.

Aftershock probabilistic seismic hazard analysis is expressed in terms of rate of events exceeding a ground motion intensity measure threshold at a site of interest. The main difference with long-term (or mainshock) PSHA [4] is that such a rate is time-variant. The expected number of events per unit time decreases as the time elapsed since the triggering event increases. In this sense, the aftershock process is conditional to the mainshock occurrence and characteristics.

In APSHA, at time t (assuming that the mainshock occurred at $t=0$), the daily rate of the aftershocks' occurrence, $\lambda(t)$, is provided in Equation (1). Aftershock magnitude is bounded between a minimum value of interest, m_l , and that of the mainshock, m_m . Coefficients a and b are from a suitable *Gutenberg–Richter relationship*, while c and p are from the *modified Omori law* for the considered sequence. From Equation (1), it follows that the expected number of aftershocks in the $(t, t + \Delta t)$ interval, is given by Equation (2), which applies for a nonhomogenous Poisson process (NHPP).

$$\lambda(t) = \left(10^{a+b \cdot (m_m - m_l)} - 10^a\right) / (t + c)^p \quad (1)$$

$$E[N(t, t + \Delta t)] = \int_t^{t+\Delta t} \lambda(\tau) \cdot d\tau = \frac{10^{a+b \cdot (m_m - m_l)} - 10^a}{p - 1} \cdot \left[(t + c)^{1-p} - (t + \Delta t + c)^{1-p}\right] \quad (2)$$

Aftershock probabilistic seismic hazard analysis *filters* the rate by the (time-invariant) probability that the ground motion intensity measure, IM , at the site of interest exceeds a threshold, $P[IM > im]$. This leads to the rate of the NHPP process, $\lambda_{im}(t)$, as in Equation (3), where $P[IM > im | m, r_s]$ is provided by a ground motion prediction equation and $f_{M,R_s}(m, r_s)$ is the joint probability density function (PDF) of magnitude and source-to-site distance, R_s , of aftershocks.[†]

[†]Ground motion prediction equations also depend on local geology. In this study, it is assumed that the aftershock sequence cannot modify site's soil properties.

$$\lambda_{im}(t) = \lambda(t) \cdot P[IM > im] = \lambda(t) \cdot \iint_{m, r_s} P[IM > im | m, r_s] \cdot f_{M, R_s}(m, r_s) \cdot dm \cdot dr_s \quad (3)$$

If only aftershocks above a certain intensity threshold, im^* , are damaging (e.g., above the intensity corresponding to the elastic limit of the structure, see the next section), Equation (3) may also serve to compute the rate of the NHPP characterizing their occurrence: $\lambda_D(t) = \lambda(t) \cdot P[IM > im^*]$.

An important feature of APSHA is that the distributions of magnitude and distance of each aftershock, neither varies among aftershocks nor with time. More rigorously speaking, M and R_s of different aftershocks are i.i.d. RVs [1]. The sequence depends on time only because of the rate of the occurrence process. Consequently, the IM s of different aftershocks are also i.i.d.

3. DAMAGE ACCUMULATION AND COLLAPSE CRITERION

Mostly in the last three decades, literature has addressed an in-depth discussion of seismic damage measures with respect to the characteristics of common structures and to the dynamic performances of larger engineering interest. According to the comprehensive review of [5], damage indices may be first categorized in two main classes as *displacement-related* and *energy-related*. In the former case, the principle is that the structure reaches collapse because it exceeds its maximum plastic displacement, that is, maximum strain, independently of the amount of dissipated energy. The latter case refers to structures in which damage is related to the amount of energy dissipated by hysteretic loops. In fact, the most representative strain-based damage index is the maximum displacement demand, while hysteretic energy (i.e., the summation of the areas of plastic cycles during seismic shaking) is the most obvious energy-based index. Hybrid damage indices, accounting for both damage phenomena by means of a combination of measures of the two kinds, also exist; the best-known is that by Park and Ang [6].

Considering a maximum-displacement-based criterion and looking at a specific loading direction, damage accumulation in two subsequent earthquakes occurs only if the maximum displacement reached in the second one is larger than the maximum in the previous one, which makes the damage increment not independent of the shaking history. Conversely, due to the features of the EPP-SDOF system response (Figure 1, left), the area of hysteretic loops during the shaking from the second shock is independent of the previous shaking demand (Figure 1, right).

In this work, damage measures based on the area of plastic cycles, and therefore on hysteretic energy, are considered as a reference. In fact, as discussed in the next section, this enables to derive reliability models based on the hypothesis that damage increments in seismic sequences are i.i.d. RVs, which practically means that, in any specific earthquake, the structure responds always in the

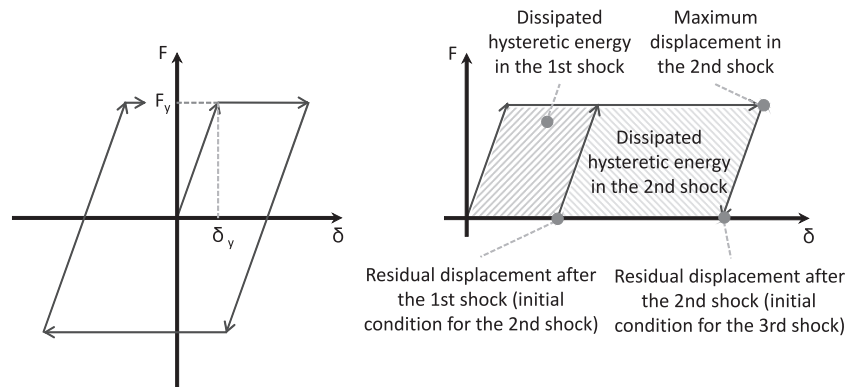


Figure 1. Elastic-perfectly-plastic nonevolutionary behavior (left) and monotonic (simplistic) scheme of cumulative response in terms of maximum displacement and dissipated hysteretic energy (right). F is the force, δ is the displacement, and y subscript indicates yielding.

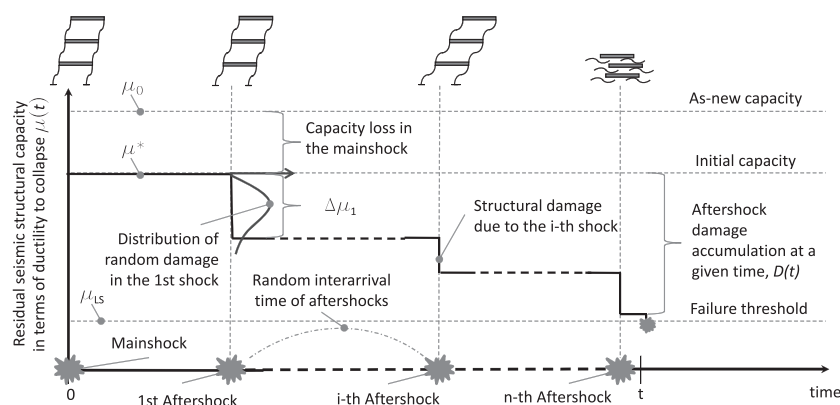


Figure 2. Degradation process for a mainshock-damaged structure exposed to aftershocks.

same manner, and independently of its status prior to the shock. As discussed, such a condition applies to the *nonevolutionary* EPP-SDOF, if any energy-related damage index is chosen [5, 7].[‡]

To focus on the reliability analysis more than on structural modeling, the *kinematic ductility*, μ (i.e., the maximum displacement demand, when the yielding displacement is the unit) is chosen as the simplest proxy for the dissipated hysteretic energy during one earthquake event. To capture energy dissipation in a single shock only, ductility is computed as if the residual displacement at beginning of each ground motion is zero. Note that this implies, as in all energy-based damage measures, structural damage in all seismic events with intensity larger than that required to yield the structure.

The collapse is assumed to occur when kinematic ductility, conservatively accumulated independently on the sign of maximum displacement, reaches some capacity value.

It is to underline, finally, that kinematic ductility may be considered as an overly simplistic proxy for dissipated hysteretic energy. In fact, more refined and less approximated energy-related indices are perfectly consistent with the adopted framework and could be considered. The chosen damage index was chosen because of its advantages in estimating structural response via nonlinear dynamic analysis. Indeed, in [7], it was demonstrated that for the EPP-SDOF, given first-mode spectral acceleration, no other ground motion characteristics needs to be considered to obtain an unbiased estimate of seismic damage when the latter is related to kinematic ductility. Benefit of this feature, for the illustrative purposes of this paper, will be more evident in Section 5.

4. GAMMA MODEL FOR THE CUMULATIVE DAMAGE PROCESS

Given a mainshock-damaged structure, aftershocks may potentially further increase damage, unless partial or total restoration. Cumulative damage, or degradation, measured for example by means of the residual ductility to collapse, or $\mu(t)$, may be susceptible of the representation as a function of time in Figure 2, which refers to a failure threshold corresponding to a limit-state of interest.

Formally, the degradation process is that in Equation (4), where μ^* is the capacity at $t=0$, immediately after the mainshock of interest, and $D(t)$ is the cumulated damage due to all aftershocks, $N(t)$, occurring within t . Both $\Delta\mu_i$ (damage in one aftershock) and $N(t)$ are RVs.

$$\mu(t) = \mu^* - D(t) = \mu^* - \sum_{i=1}^{N(t)} \Delta\mu_i \quad (4)$$

Given this formulation, the probability the structure fails within time t , $P_f(t)$, is the probability that the structure passes the limit-state threshold, μ_{LS} , or the complement to one of reliability, $R(t)$, Equation (5). In

[‡]Measures as that of [6] do not allow to have independent damage increments. However, some authors (i.e., [22]) seem to apply the Park and Ang index in a way that i.i.d. hypothesis in seismic sequences is retained.

fact, it is the probability that the cumulated damage is larger than the difference between the initial value and the threshold, $\bar{\mu} = \mu^* - \mu_{LS}$.

$$P_f(t) = 1 - R(t) = P[\mu(t) \leq \mu_{LS}] = P[D(t) \geq \mu^* - \mu_{LS}] = P[D(t) \geq \bar{\mu}] \quad (5)$$

In the case, the occurrence of seismic shocks is described by a NHPP, and considering the cumulated damage as dependent on the random vector of the ground motion intensity measures of consecutive aftershocks, \underline{IM} , then $P_f(t)$ may be computed from Equation (6), where the integral is of k -th order.

$$\begin{aligned} P_f(t) &= \sum_{k=1}^{+\infty} P[D(t) \geq \bar{\mu} | N(t) = k] \cdot P[N(t) = k] = \\ &= \sum_{k=1}^{+\infty} \int P \left[\sum_{i=1}^k \Delta \mu_i \geq \bar{\mu} | \underline{IM} = \underline{im}, N(t) = k \right] \cdot f_{\underline{IM}}(\underline{im}) \cdot d(\underline{im}) \cdot \frac{(E[N(t)])^k}{k!} e^{-E[N(t)]} \end{aligned} \quad (6)$$

Because it was shown in Section 2 that IM s from APSHA, for example first-mode spectral acceleration, or Sa , in different earthquakes are i.i.d. RVs, then $f_{\underline{IM}}(\underline{im})$ is simply the product of $f_{IM_i}(im)$ distributions, which are k in number. Therefore, the critical issue to compute the probability of failure is to obtain $P[D(t) \geq \bar{\mu} | \underline{IM} = \underline{im}, N(t) = k]$, that is, the probability of cumulative damage exceeding the threshold conditional to intensities and number of shocks. Alternatively, considering the first line of Equation (6) and because $P[N(t)=k]$ is provided by a Poisson distribution of rate $\lambda(t)$, then $P[D(t) \geq \bar{\mu} | N(t) = k]$ is sufficient to solve the reliability problem. This latter strategy is adopted in the following.

4.1. Damage increments characterization and absolute reliability approximation

Reliability assessment may be easily addressed if three conditions are met [8]:

1. damages produced in different events are independent RVs;
2. damage in the i -th earthquake, $\Delta \mu_i$, has always the same distribution, $f_{\Delta \mu_i}(\delta \mu)$, marginal with respect to \underline{IM} , that is, $f_{\Delta \mu_i}(\cdot) = f_{\Delta \mu}(\cdot) \forall i$;
3. the distribution of sums of damages can be expressed in a simple form.

According to conditions (1) and (2), earthquakes' structural effects are i.i.d.[§] A way to satisfy condition (3) consists of modeling damage via a RV that enjoys the *reproductive* property. A well-known example of reproductive RV is the Gaussian one. However, because it should be $\Delta \mu_i \geq 0 \forall i$, the cumulative degradation process due to subsequent aftershocks should show nonnegative increments, disqualifying the Gaussian representation of damage. Although the lognormal PDF may appear as a solution, it is not reproductive in the addition sense. In fact, an attractive option to probabilistically model damage increment is the gamma distribution. This distribution, shown at the right hand side of Equation (7), is used in this study to model the damage in a single earthquake, that is, the marginalization of structural damage conditional to seismic intensity with the distribution of \underline{IM} in one aftershock. In other words, it is the PDF of damage in an individual aftershock event, considering all its possible ground motion intensities and reflecting their relative probabilities.

It may be seen from Equation (7) that the gamma distribution depends on γ_D and α_D , which are the scale and shape parameters, respectively. This PDF is quite flexible: a shape parameter equal to one, stretches the distribution to the exponential; a large value of α_D , say larger than four, let the PDF be similar to that Gaussian; an intermediate value, around two, makes it similar to the lognormal shape.

[§]This, in particular, implies increment of damage in an earthquake is independent of structural state. Otherwise, for example in the case of systems with evolutionary or degrading hysteretic behavior, *state-dependent* approaches may be required [23–25].

The D subscript in this equation (and in all those following) emphasizes that, being continuous and nonnegative, such RV is suitable to model only the effect of earthquakes factually determining loss of capacity, not those events whose intensity is not large enough (Section 3).

$$f_{\Delta\mu}(\delta\mu) = \int_{im} f_{\Delta\mu|IM}(\delta\mu|x) \cdot f_{IM}(x) \cdot dx \triangleq \frac{\gamma_D \cdot (\gamma_D \cdot \delta\mu)^{\alpha_D-1}}{\Gamma(\alpha_D)} \cdot e^{-\gamma_D \cdot \delta\mu} \quad (7)$$

Because the sum of k_D i.i.d. gamma-distributed RVs, with scale and shape parameters γ_D and α_D respectively, is still gamma with parameters γ_D and $k_D \cdot \alpha_D$, then the probability of cumulative damage exceeding the threshold, conditional to k_D shocks, is given by Equation (8), where $N_D(t)$ is the NHPP counting function for the damaging events and, as shown in the Appendix, $\Gamma(\beta)$ and $\Gamma_U(\beta, y)$ are the *gamma* and the *upper incomplete gamma* functions, respectively.

$$P[D(t) \geq \bar{\mu} | N_D(t) = k_D] = \int_{\bar{\mu}}^{+\infty} \frac{\gamma_D \cdot (\gamma_D \cdot x)^{k_D \cdot \alpha_D - 1}}{\Gamma(k_D \cdot \alpha_D)} \cdot e^{-\gamma_D \cdot x} \cdot dx = \frac{\Gamma_U(k_D \cdot \alpha_D, \gamma_D \cdot \bar{\mu})}{\Gamma(k_D \cdot \alpha_D)} \quad (8)$$

At this point, the convenient *first moment approximation* is worth to be introduced. If $P_f(t)$ is computed as per the first line of Equation (6), it consists of replacing the entire summation only with the term conditional to the expected number of damaging earthquakes until t , which yields Equation (9). These kinds of approximations, whose tolerability will be addressed with respect to the illustrative application in Section 5, are generally referred to as the *delta method* [9].

$$\begin{aligned} P_f(t) &= \sum_{k=1}^{+\infty} P[D(t) \geq \bar{\mu} | N_D(t) = k] \cdot P[N_D(t) = k] \approx P[D(t) \geq \bar{\mu} | N_D(t) = E[N_D(t)]] = \\ &= \int_{\bar{\mu}}^{+\infty} \frac{\gamma_D \cdot (\gamma_D \cdot x)^{E[N_D(t)] \cdot \alpha_D - 1}}{\Gamma(E[N_D(t)] \cdot \alpha_D)} \cdot e^{-\gamma_D \cdot x} \cdot dx = \frac{\Gamma_U(E[N_D(t)] \cdot \alpha_D, \gamma_D \cdot \bar{\mu})}{\Gamma(E[N_D(t)] \cdot \alpha_D)} \end{aligned} \quad (9)$$

The failure probability as per Equation (9) allows a closed-form solution of the reliability problem as the expected number of aftershocks may be provided by Equation (2).

4.2. Conditional reliability given different information on the structural history

Assume one wants, during the sequence, to include in the reliability assessment the information that the structure is still surviving at a certain time after the mainshock, t_1 , but with unknown damage conditions due to aftershocks. It may be computed via Equation (10), being one minus the probability of surviving at t divided by the probability the structure is above the failure threshold at t_1 . Also to compute this conditional failure probability, the first moment approximation was considered, while marginalization with respect to the number of occurring aftershocks is required to obtain the exact result.

Another approximate conditional probability of failure that may be obtained in closed-form is that conditional on the following information: (i) the structure surviving at t_1 and (ii) it has been already subjected to a given number, k_D , of damaging aftershocks. This is given in Equation (11) as one minus the reliability due to shocks until t , which includes those (k_D in number) occurred until t_1 and those that will occur in the (t_1, t) interval, divided by the reliability conditional to the k_D aftershocks, whose occurrence is certain.

Even if ugly looking, these equations allow a simple reliability assessment, as shown in the next section, because numerical solutions are readily available for the gamma functions.

$$\begin{aligned}
P_{f|D(t_1) < \bar{\mu}}(t) &= 1 - \frac{R(t)}{R(t_1)} = 1 - \frac{1 - P_f(t)}{1 - P_f(t_1)} \approx 1 - \frac{1 - P[D(t) \geq \bar{\mu} | N_D(t) = E[N_D(t)]]}{1 - P[D(t_1) \geq \bar{\mu} | N_D(t_1) = E[N_D(t_1)]]} = \\
&= 1 - \frac{1 - \int_{\bar{\mu}}^{+\infty} \frac{\gamma_D \cdot (\gamma_D \cdot x)^{E[N_D(t)] \cdot \alpha_D - 1}}{\Gamma(E[N_D(t)] \cdot \alpha_D)} \cdot e^{-\gamma_D \cdot x} \cdot dx}{1 - \int_{\bar{\mu}}^{+\infty} \frac{\gamma_D \cdot (\gamma_D \cdot x)^{E[N_D(t_1)] \cdot \alpha_D - 1}}{\Gamma(E[N_D(t_1)] \cdot \alpha_D)} \cdot e^{-\gamma_D \cdot x} \cdot dx} = 1 - \frac{1 - \frac{\Gamma_U(E[N_D(t)] \cdot \alpha_D, \gamma_D \cdot \bar{\mu})}{\Gamma(E[N_D(t)] \cdot \alpha_D)}}{1 - \frac{\Gamma_U(E[N_D(t_1)] \cdot \alpha_D, \gamma_D \cdot \bar{\mu})}{\Gamma(E[N_D(t_1)] \cdot \alpha_D)}} \quad (10)
\end{aligned}$$

$$\begin{aligned}
P_{f|D(t_1) < \bar{\mu}, N_D(t_1) = k_D}(t) &= 1 - \frac{1 - P\left[\sum_{i=1}^{k_D + N_D(t_1, t)} \Delta \mu_i \geq \bar{\mu}\right]}{1 - P\left[\sum_{i=1}^{k_D} \Delta \mu_i \geq \bar{\mu}\right]} \approx \\
&\approx 1 - \frac{1 - \int_{\bar{\mu}}^{+\infty} \frac{\gamma_D \cdot (\gamma_D \cdot x)^{(k_D + E[N_D(t_1, t)]) \cdot \alpha_D - 1}}{\Gamma[(k_D + E[N_D(t_1, t)]) \cdot \alpha_D]} \cdot e^{-\gamma_D \cdot x} \cdot dx}{1 - \int_{\bar{\mu}}^{+\infty} \frac{\gamma_D \cdot (\gamma_D \cdot x)^{k_D \cdot \alpha_D - 1}}{\Gamma(k_D \cdot \alpha_D)} \cdot e^{-\gamma_D \cdot x} \cdot dx} \quad (11) \\
&= 1 - \frac{1 - \frac{\Gamma_U[(k_D + E[N_D(t_1, t)]) \cdot \alpha_D, \gamma_D \cdot \bar{\mu}]}{\Gamma[(k_D + E[N_D(t_1, t)]) \cdot \alpha_D]}}{1 - \frac{\Gamma_U(k_D \cdot \alpha_D, \gamma_D \cdot \bar{\mu})}{\Gamma(k_D \cdot \alpha_D)}}
\end{aligned}$$

5. ILLUSTRATIVE APPLICATION

The application refers to a simple EPP-SDOF system with reloading/unloading stiffness, which is the same as the initial one (Figure 1, left). The elastic period is equal to 0.5 s; weight is 100 kN, and the yielding force is equal to 19.6 kN.

Following Section 3, the chosen engineering demand parameter is the kinematic ductility, μ , that is, the maximum displacement demand, when the yielding displacement is the unit. The system, in its initial (undamaged) state, is assumed to have a ductility capacity $\mu_0 = 3.3$, and each damaging shock drains some of this ductility supply (Figure 3).[§]

As discussed, the considered system shows stable hysteretic cycles that repeat themselves despite of the sequence of excitation it undergoes to, which is important with respect to the reliability models based on i.i.d. damage increments. In fact, the force-deformation response is such that the ductility demand in the i -th earthquake of a sequence is just the same as if the damaging event hit the structure in initial conditions. In other words, *variation* of drained capacity measured in terms of ductility (proxy for energy dissipation) in the i -th earthquake is independent of the state the shock finds the structure in. Thus, considering that ground motion intensities in different aftershocks are also i.i.d. (Section 2), damage increments are clearly i.i.d., as both seismic input and considered structural response in one shock have always the same characteristics and are independent of what happened previously. In the following subsection, a gamma distribution is calibrated for the damage increment of the EPP-SDOF considered.

[§]The capacity was obtained as the ductility corresponding to the drift threshold for the onset of *collapse prevention* limit-state for reinforced concrete frames in [26], that is 0.04. This is to obtain a purely conventional measure of energy dissipation structural supply, which may be not perfectly appropriate if such a threshold refers to a maximum displacement collapse criterion.

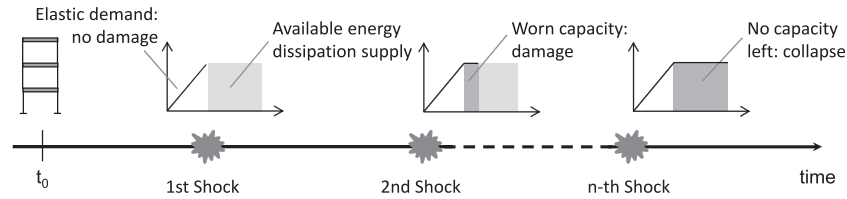


Figure 3. Accumulation of damage with respect to kinematic ductility for elastic-perfectly-plastic systems.

5.1. Calibrating the gamma distribution for damage increments

The PDF of damage in a shock may be obtained via the marginalization in Equation (7). It first requires f_{IM} , that is, the distribution of ground motion intensity *given the occurrence of an aftershock*. Assuming S_a at the elastic period of the SDOF as an IM , f_{IM} was computed via the integral term at the right hand side of Equation (3). The M and R_s RVs were considered to be stochastically independent in one aftershock.

Following from Section 2, $f_M(m)$ is considered to be an exponential PDF with the upper bound of magnitude equal to 6.3, which corresponds to the 2009 L'Aquila (central Italy) earthquake magnitude. The minimum aftershock magnitude value was arbitrarily taken equal to 4.3. The b -value of the Gutenberg–Richter relationship was taken equal to 0.96, as justified in the following subsection.

To constrain the epicenters of aftershocks, a 400 km² aftershock source area around the site was considered (Figure 4(a)). Therefore, f_{R_s} only accounts for such a seismogenic zone; the size of which was obtained by the aftershock area versus mainshock magnitude relationship in [10].

In fact, the structure may be considered located in L'Aquila (13.40 longitude, 42.35 latitude), Figure 4(a), even if all assumptions of the application are generic, and reference to the 2009

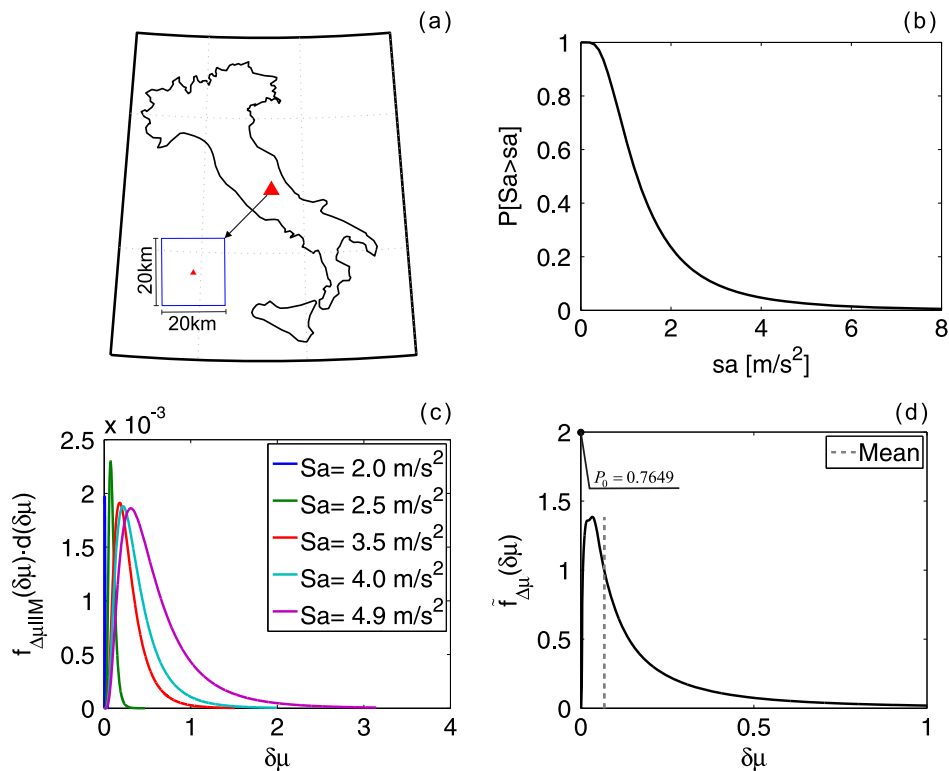


Figure 4. (a) Considered site (triangle) and the seismic source zone for aftershocks; (b) distribution of S_a (0.5 s) given the occurrence of an aftershock according to the assumptions taken in the illustrative application; (c) examples of distribution of structural damage conditional to ground motion intensity; and (d) distribution of damage to the structure due to an aftershock of any possible intensity.

earthquake is only in terms of mainshock magnitude. (It is to note, however, that the aftershock area considered is not much larger than the fault supposed to have originated the 2009 earthquake [11].)

Figure 4(b) shows the resulting f_{IM} ; the hazard software and ground motion prediction equation used for the calculations were the same of [12].

The probabilistic seismic demand term, $f_{\Delta\mu/IM}$, may be computed via *incremental dynamic analysis* (IDA).[‡] Seismic demand analysis was developed in terms of structural ductility response normalized by μ_0 (Figure 2), so that demand is equal to 1 at onset of failure. Indeed, damage in a single shock is defined as per Equation (12), where μ_{before} and μ_{after} refer to capacity before and after the generic aftershock. Figure 4(c) shows $f_{\Delta\mu/IM}$ for some ground motion intensities under the, formally tested, lognormal assumption.

$$\Delta\mu = \frac{\mu_{before} - \mu_{after}}{\mu_0} \quad (12)$$

To develop IDAs, 30 records were selected via REXEL [13], with moment magnitude between 5 and 7, epicentral distances lower than 30 km, and stiff site class. It is to note that no special attention was put in the selection of records to estimate response of the structure to aftershocks, neither in terms of magnitude and source-to-site distance nor in making sure they are identified as aftershocks of a specific main event. Two related reasons explain why in evaluating $f_{\Delta\mu/IM}$ it was not needed to simulate specific *mainshock–aftershock sequences* (e.g., [14]). First, it is to recall that the PDF of damage in a single aftershock is the target; it is the combination of aftershock hazard and structural response as per Equation (7). In the equation, the f_{IM} term represents the PDF of Sa in one aftershock (equal for all aftershocks according to APSHA) and provides all necessary information on the aftershock intensity to evaluate structural response. Indeed, the $f_{\Delta\mu/IM}$ term may be estimated as commonly performed via IDAs, in which simply the distribution of structural response, given first-mode spectral acceleration, is sought. Second, because kinematic ductility for an EPP-SDOF system is considered as the engineering demand parameter, neither special care has to be taken in selecting records from specific magnitude-distance bins [15, 16] nor other ground motion features, such as duration, matter [7]. This is because, to estimate kinematic ductility demand, first-mode spectral acceleration may be considered a *sufficient IM* [17].

Nevertheless, in the case of other damage measures for which Sa is not sufficient and other ground motion characteristics need to be taken into account (see [7] for a discussion), APSHA can be extended to provide vector-valued hazard and/or seismic demand analysis can consider explicitly these issues deemed relevant to structural response [18, 19].

The marginalization as per Equation (7) leads to the distribution of damage in Figure 4(d). To comment such a plot, it has to be recalled that not all aftershocks are strong enough to yield the structure and $\Delta\mu = 0$ in the case of *weak* motions. In particular, $\Delta\mu$ is larger than zero only for first-mode spectral accelerations larger than 1.96 m/s^2 , that is, the yielding acceleration of the considered EPP-SDOF. Thus, damage in one shock is not a continuous RV, and its cumulative distribution function has the expression in Equation (13). In other words, the distribution of $\Delta\mu$ is defined by means of a probability density for $\Delta\mu > 0$ and a *probability mass* in zero. In fact, $P_0 = P[\Delta\mu = 0]$ accounts for the probability that shocks are not strong enough to damage the structure. In this case, P_0 is equal to 0.7649, that is, only 23.5% of aftershocks, occurring in the considered area and magnitude bounds, is expected to be damaging. In Figure 4(d), the mean of the damage increment (dashed vertical line), accounting for both damaging and undamaging aftershocks, is also given.

$$P[\Delta\mu \leq \delta\mu] = \begin{cases} P_0 & \delta\mu = 0 \\ P_0 + \int_0^{\delta\mu} \tilde{f}_{\Delta\mu}(x) \cdot dx & \delta\mu > 0 \end{cases} \quad (13)$$

[‡]In fact, due to the mentioned repetitive features of the EPP response, it is also easy to show that a single set of IDAs is needed to estimate the distribution of damage increment given IM , see [27] for details.

Average degradation increment due to a damaging aftershock, $E[\Delta\mu|\Delta\mu > 0]$, is 0.2884, while the variance, $Var[\Delta\mu|\Delta\mu > 0]$, is 0.3522. To retain such moments, the gamma PDF adopted to model the shock effect in the case of damage larger than zero, $f_{\Delta\mu}(\delta\mu) = \tilde{f}_{\Delta\mu}(\delta\mu)/(1 - P_0)$, must have scale and shape parameters equal to 0.8187 and 0.2361, respectively. This is because the mean and the variance in the gamma distribution are equal to α_D/γ_D and α_D/γ_D^2 , respectively.

5.2. Reliability in the aftershock sequence of an M 6.3 mainshock

Risk assessment as per the developed model first requires the rate, $\lambda(t)$, of aftershocks from Equation (1). To this aim, coefficients of the *generic sequence* from [20] were used: $a = -1.66$, $b = 0.96$, $c = 0.03$, and $p = 0.93$. Bounding magnitudes, m_l and m_m , were assigned in the previous section, that is, 4.3 and 6.3, respectively. Then, the (filtered) rate of damaging aftershocks is $\lambda_D(t) = \lambda(t) \cdot P[\Delta\mu > 0] = \lambda(t) \cdot (1 - 0.7649)$. Thus, the expected number of damaging events, in any time interval, is given by Equation (2), in which $\lambda_D(t)$ replaces $\lambda(t)$. Figure 5(a) plots the total and damaging aftershock rates until 3 months since the mainshock.

It was arbitrarily assumed that the structure has survived to the mainshock event with a residual capacity $\mu^* = 0.7$ (i.e., 30% capacity reduction). Before proceeding any further, it is to underline that estimation of capacity reduction after a mainshock, an input for the reliability models, is a relevant and nontrivial issue in earthquake engineering. Luco *et al.* [21] list three alternative ways for identifying the post-event building damage state: (i) combination of fragility curves of undamaged building with shake-maps, which are usually available right after the mainshock; (ii) inspection; and (iii) analysis of the structural information provided by a health monitoring systems (if available). Quantitative approaches (i) and (iii) appear more compatible with the framework of this study, which requires quantitative assessment of damage. Alternatively, expected capacity reduction in the

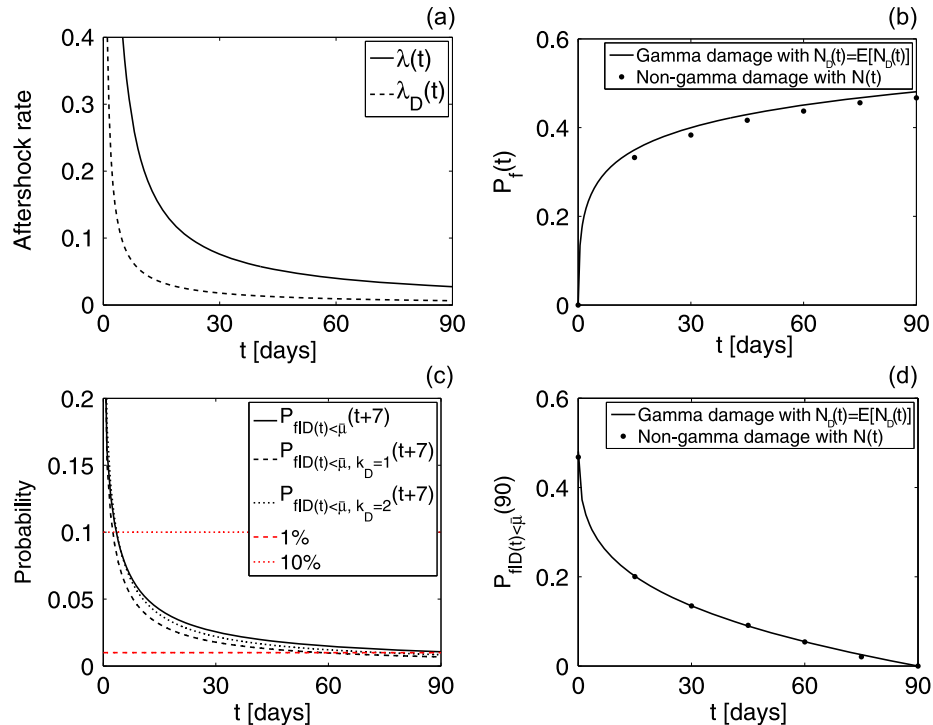


Figure 5. (a) Total and damaging aftershock rates within 90 days since the mainshock; (b) failure probability for the structure as time since the mainshock passes; (c) failure probability in the 7 days following t given survival at t , and possibly occurrence of damaging aftershocks; and (d) failure probability in what remains of 3 months since the mainshock (90- t), given survival at t .

main event can be obtained by means of a model of the type in Equation (7), in which f_{IM} is replaced by the IM distribution conditional to magnitude and source-to-site distance of the mainshock.

Once the starting seismic capacity is known, the failure probabilities according to the models of Section 4.1 can be easily computed via, for example, the *gammainc* function implemented in MATHWORKS-MATLAB®. The following cases, reported in panels (b)–(d) of Figure 5, were addressed for the purpose of illustration. In the figure, t is always the time since the mainshock.

- Figure 5(b): absolute failure probability in the $(0, t)$ interval from Equation (9). The trend is increasing with time passed since the mainshock because the larger the interval, the larger the expected number of shocks, which may cumulate damage on the structure leading to collapse.
- Figure 5(c): this panel shows three curves:
 - $P_{f|D(t) < \bar{\mu}}(t + 7)$ from Equation (10), that is, the failure probability of the structure in 1 week after t , given survival at the time of reliability assessment;
 - $P_{f|D(t) < \bar{\mu}, k_D=1}(t + 7)$ from Equation (11), that is, the failure probability given survival in t and the information that one damaging aftershocks has occurred previous to the time of the reliability evaluation;
 - $P_{f|D(t) < \bar{\mu}, k_D=2}(t + 7)$, that is, the same as per the previous case except that it is known that two damaging aftershocks have occurred before t .
- Figure 5(d): $P_{f|D(t) < \bar{\mu}}(90)$ from Equation (10), that is, assuming 3 months as reference duration of the sequence, the failure probability in the remaining exposure time $(90 - t)$, given survival in t .

As an illustration of use of these results, Figure 5(c) also reports two (time-invariant) risks. The lower one is 1%, the larger one is 10%. Following the approach in [3] and arbitrarily assuming the probability 1% as a tolerable collapse risk in 1 week during an aftershock sequence and 10 times its value as a tolerable risk for emergency operations, it may be said that before the decaying risk intersects the largest probability, the structures is red tagged (i.e., cannot be accessed) in the next week, is green tagged after the aftershock risk gets smaller than the lower value, and can be entered only by trained agents in between.

Finally, dotted graphs in Figure 5(b) and (d) represent the same results as per the solid lines, yet computed, via Monte Carlo simulation, removing the hypothesis that increments are gamma-distributed and without using the first moment approximation, that is, directly employing Equation (6). It appears that, at least in this case, errors introduced by the approximated models appear tolerable and on the safe side.

6. CONCLUSIONS

Starting from APSHA, closed-form models for the reliability assessment of damage-cumulating EPP systems in aftershock environment were developed and discussed. They are based on a cumulative shock model, which makes use of the gamma distribution to describe structural seismic damage in a shock of any possible intensity, and nonhomogeneous Poisson process probabilistically modeling occurrence of shocks, as per APSHA.

A required feature of structural damage is that it is represented by means of RVs that are i.i.d. in different earthquakes and independent on the history of the sequence. This was found to be the case for the considered structural system when energy-based damage measures are considered. To this aim, kinematic ductility was considered as a proxy (intentionally simplistic) for dissipated hysteretic energy during one aftershock.

The stochastic degradation process, descending from these hypotheses, is an independent increments one. It enables approximate closed-form solutions for absolute reliability, as well as conditional to different information about the structure, namely (i) knowledge of survival and unknown residual capacity and (ii) knowledge of survival, known number of already occurred damaging aftershock, and unknown residual capacity. The models also explicitly account for the fact that the majority of aftershocks are expected to be undamaging for the structure.

The applicability of the models was illustrated via an example referring to a mainshock-damaged system, supposed to be subjected to a generic aftershock sequence following an M 6.3 event. Different kinds of failure risks during the sequence were evaluated. Some of them were also compared with

arbitrary values of tolerable risk, which were used as tagging criteria in a virtual application of short-term seismic risk management.

The results from the model were also discussed with respect to approximations invoked, which appear tolerable, if compared with the rapid risk assessment the closed-forms allow.

APPENDIX

The *gamma* and the *upper incomplete gamma* functions as in Equations (A.1) and (A.2), respectively.

$$\Gamma(\beta) = \int_0^{+\infty} z^{\beta-1} \cdot e^{-z} \cdot dz \quad (\text{A.1})$$

$$\Gamma_U(\beta, y) = \int_y^{+\infty} z^{\beta-1} \cdot e^{-z} \cdot dz \quad (\text{A.2})$$

Assigning $\beta = k_D \cdot \alpha_D$ and $z = \gamma_D \cdot x$, then it results $dz = \gamma_D \cdot dx$ and $y = \gamma_D \cdot \bar{\mu}$ from which Equations (A.3) and (A.4), used in the paper, may be derived.

$$\Gamma(k_D \cdot \alpha_D) = \int_0^{+\infty} \gamma_D (\gamma_D \cdot x)^{k_D \cdot \alpha_D - 1} \cdot e^{-\gamma_D \cdot x} \cdot dx \quad (\text{A.3})$$

$$\Gamma_U(k_D \cdot \alpha_D, \gamma_D \cdot \bar{\mu}) = \int_{\bar{\mu}}^{+\infty} \gamma_D \cdot (\gamma_D \cdot x)^{k_D \cdot \alpha_D - 1} \cdot e^{-\gamma_D \cdot x} \cdot dx \quad (\text{A.4})$$

These functions have the advantage to feature tabular solution available; therefore, convenience in expressing the failure probability in these terms may be argued.

ACKNOWLEDGEMENTS

This research was developed in the framework of *Analisi e Monitoraggio dei Rischi Ambientali scari* (AMRA) (<http://www.amracenter.com>), partially within the *Strategies and tools for Real-Time Earthquake Risk Reduction* (REAKT; <http://www.reaktproject.eu>) project, and partially within the New Multi-Hazard and Multi-Risk Assessment Methods for Europe (MATRIX; <http://matrix.gpi.kit.edu/>) project. Both funded by the European Community via the Seventh Framework Program for Research (FP7), with contracts nos. 282862 and 265138, respectively. The authors want also to acknowledge the comments of the reviewers, whose comments significantly improved quality and readability of the paper.

REFERENCES

1. Yeo GL, Cornell CA. A probabilistic framework for quantification of aftershock ground-motion hazard in California: methodology and parametric study. *Earthquake Engineering and Structural Dynamics* 2009; **38**(1): 45–60.
2. Yeo GL, Cornell CA. Post-quake decision analysis using dynamic programming. *Earthquake Engineering and Structural Dynamics* 2009; **38**(1):79–93.
3. Yeo GL, Cornell CA. Stochastic characterization and decision bases under time-dependent aftershock risk in performance-based earthquake engineering, PEER Report 2005/13, Pacific Earthquake Engineering Research Center, Berkeley, CA, 2005.
4. McGuire RK. *Seismic Hazard and Risk Analysis*, Earthquake Engineering Research Institute, MNO-10: Oakland, CA, 2004.
5. Cosenza E, Manfredi G. Damage indices and damage measures. *Progress in Structural Engineering and Materials* 2000; **2**(1):50–59.
6. Park Y, Ang A. Mechanistic seismic damage model for reinforced concrete. *Journal of Structural Engineering* 1985; **111**(4):722–739.
7. Iervolino I, Manfredi G, Cosenza E. Ground motion duration effects on nonlinear seismic response. *Earthquake Engineering and Structural Dynamics* 2006; **35**(1):21–38.
8. Iervolino I, Chioccarelli E, Giorgio M. Time-dependent seismic reliability of damage-cumulating non-evolutionary bilinear systems. Proc. of 15th World Conference on Earthquake Engineering, Lisbon, Portugal, 2012. Paper No. 2893.
9. Oehlert GW. A note on the delta method. *The American Statistician* 1992; **46**(1):27–29.

10. Utsu T. Aftershocks and earthquake statistics (1): some parameters which characterize an aftershock sequence and their interrelations. *Journal of the Faculty of Science, Hokkaido University, Series 7, Geophysics* 1970; **3**(3):129–195.
11. Chioccarelli E, Iervolino I. Near-source seismic demand and pulse-like records: a discussion for L'Aquila earthquake. *Earthquake Engineering and Structural Dynamics* 2010; **39**(9):1039–1062.
12. Iervolino I, Chioccarelli E, Convertito V. Engineering design earthquakes from multimodal hazard disaggregation. *Soil Dynamics and Earthquake Engineering* 2011; **31**(9):1212–1231.
13. Iervolino I, Galasso C, Cosenza E. REXEL: computer aided record selection for code-based seismic structural analysis. *Bulletin of Earthquake Engineering* 2010; **8**(2):339–362.
14. Goda K, Taylor CA. Effects of aftershocks on peak ductility demand due to strong ground motion records from shallow crustal earthquakes. *Earthquake Engineering and Structural Dynamics* 2012; **41**(15): 2311–2330.
15. Shome N, Cornell CA, Bazzurro P, Carballo JE. Earthquakes, records, and nonlinear responses. *Earthquake Spectra* 1998; **14**(3):469–500.
16. Iervolino I, Cornell CA. Record selection for nonlinear seismic analysis of structures. *Earthquake Spectra* 2005; **21**(3):685–713.
17. Luco N, Cornell CA. Structure-specific scalar intensity measures for near-source and ordinary earthquake ground motions. *Earthquake Spectra* 2007; **23**(2):357–392.
18. Iervolino I, Giorgio M, Galasso C, Manfredi G. Conditional hazard maps for secondary intensity measures. *Bulletin of the Seismological Society of America* 2010; **100**(6):3312–3319.
19. Baker JW. Probabilistic structural response assessment using vector-valued intensity measures. *Earthquake Engineering & Structural Dynamics* 2007; **36**(13):1861–1883.
20. Lolli B, Gasperini P. Aftershocks hazard in Italy Part I: Estimation of time-magnitude distribution model parameters and computation of probabilities of occurrence. *Journal of Seismology* 2003; **7**(2):235–257.
21. Luco N, Gerstenberger M, Uma S, Ryu H, Liel A, Raghunandan M. A methodology for post-mainshock probabilistic assessment of building collapse risk. Proc. of the 9th Pacific Conference on Earthquake Engineering, Auckland, New Zealand; 2011.
22. Zhai C-H, Wen W-P, Chen Z, Li S, Xie L-L. Damage spectra for the mainshock–aftershock sequence-type ground motions. *Soil Dynamics and Earthquake Engineering* 2013; **45**:1–12.
23. Luco N, Cornell CA, Yeo GL. Annual limit-state frequencies for partially-inspected earthquake-damaged buildings. *Structural Safety* 2002; **24**(2–4):281–296.
24. Giorgio M, Guida M, Pulcini G. An age- and state-dependent Markov model for degradation processes. *IIE Transactions* 2011; **43**(9):621–632.
25. Giorgio M, Guida M, Pulcini G. A state-dependent wear model with an application to marine engine cylinder liners. *Technometrics* 2010; **52**(2):172–187.
26. Federal Emergency Management Agency. Prestandard and commentary for the seismic rehabilitation of buildings. Report FEMA 356. Washington DC, US, 2000.
27. Chioccarelli E, Iervolino I. In impact of repeated events with various intensities on the fragility functions for a given building typology at local scale. D4.1 of the MATRIX project, 2012. (URL <http://matrix.gpi.kit.edu/>).